RSC Advances

RSC Advances

www.rsc.org/advances

ROYAL SOCIETY
OF CHEMISTRY

www.rsc.org/advances

Mesoporous nickel phosphate-phosphonate microspheres were synthesized through a template-free phosphate-mediated self-assembly procedure, exhibiting excellent performance for capture of CO_2, adsorption of heavy metal ions like Pb^{2+}, Cu^{2+}, and Cd^{2+}, and catalytic hydrogenation of 4-nitrophenol to 4-aminophenol.
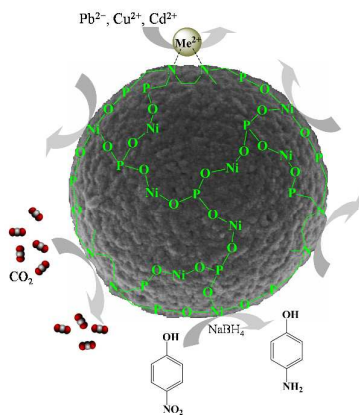
ARTICLE TYPE

Mesoporous nickel phosphate/phosphonate hybrid microspheres with excellent performance for adsorption and catalysis†

Yun-Pei Zhu,[a] Ya-Lu Liu,[a] Tie-Zhen Ren,[b] and Zhong-Yong Yuan[a],*

Mesoporous nickel phosphate/phosphonate hybrid microspheres with the combined merits of inorganic and organic components were prepared by a facile phosphate-mediated self-assembly methodology, exhibiting fine
10 **capabilities for CO$_2$ capture, heavy metal ion removal and catalytic hydrogenation of 4-nitrophenol to 4-aminophenol under ambient conditions.**

Well-structured morphology of mesoporous nanomaterials is of great importance for practical applications. Mesoporous metal
15 phosphonates, as a subset of inorganic-organic hybrid materials, have received much attention due to the combined superiorities of both inorganic units and organic moieties, showing promising applications in the field of adsorption/separation, sensors, catalysis, energy conversion and storage, biotechnoly.[1] However,
20 the morphology control is still a challenge due to the uncontrollably rapid hydrolysis rate of precursors and amorphous nature of most phosphonates.[2] Since spherical morphologies have the potential as advanced materials in designed catalysts, emission control, drug delivery, owing to the structural features
25 (*e.g.*, fine dispersity, porosity, composition, adsorption properties),[3] the aerosol methods that couple colloid chemistry and fast drying process were utilized to prepare mesoporous phosphonate-based microspheres.[4,5] Sol-gel-mediated microemulsion could also be employed to obtain mesostructured
30 titanium phosphonate microspheres with homogeneously distributed organophosphonate units in the hybrid framework.[6] Nonetheless, the preparation procedures through aerosol- or emulsion-mediated methods are complicated, and post-treatment of eliminating the surfactants may cause the collapse of
35 frameworks and even detrimentally introduce some impurities.

Self-assembly usually involves noncovalent or weak covalent interactions for promoting the disordered morphologies of materials into ordered ones, thereby simplifying the synthesis technology.[7] In this contribution, on the basis of insolubility of
40 nickel phosphate in water, a facile phosphate-mediated synthesis of mesoporous nickel phosphate/phosphonate microspheres was carried out by the template-free self-assembly methodology with the use of ethylene diamine tetra(methylene-phosphonic acid) (EDTMP, Fig. S1, ESI†) as the coupling molecule. The resultant
45 microspherical hybrids exhibited excellent capacities for CO$_2$ capture, heavy metal ion adsorption and catalytic hydrogenation of 4-nitrophenol (4-NP) to 4-aminophenol (4-AP) with the assistance of NaBH$_4$ under ambient conditions.
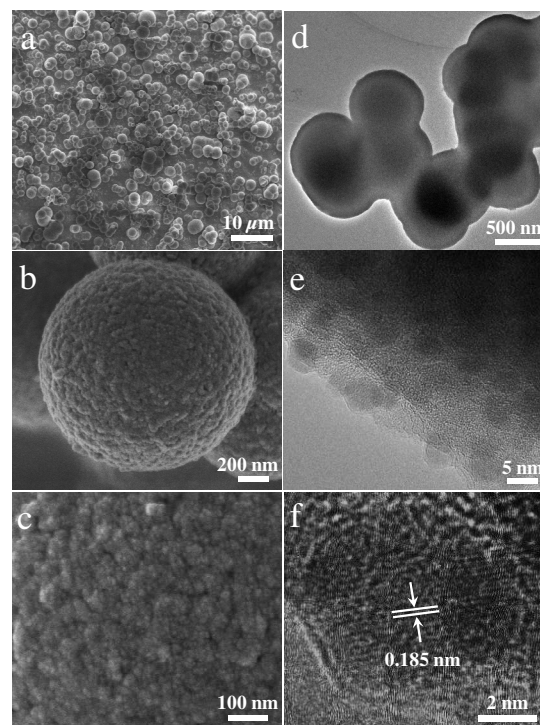

50 **Fig. 1** SEM (a, b, c) and TEM (d, e, f) images of the NiPPH material.

The mesoporous nickel phosphate/phosphonate hybrid material was prepared by the addition of EDTMP into the mixed solution of nickel salts and phosphoric acid, followed by autoclaving for a period of time, and the obtained nickel phosphate/phosphonate
55 hybrid was denoted as NiPPH. The low-magnification SEM image of NiPPH demonstrates well-structured spherical morphology of 0.4–3.5 *μ*m in size with high yield (Fig. 1a). The high-magnification image shows that the surface of the hybrid microspheres is rough (Fig. 1b). A deeper magnification (Fig. 1c)
60 illustrates that the spheres are constructed by compact aggregation of nanoparticles of about tens nanometers, giving some interpartical mesopores that may be beneficial to adsorption and catalytic reactions. TEM image shows that microspheres are of 0.5–1.2 *μ*m and some of them aggregated with each other (Fig.
65 1d). As observed from the magnified rim of a single microsphere (Fig. 1e), numerous uniform crystalline nanoparticles of 4–8 nm are homogeneously imbeded in the amorphous spheres. Fig. 1f shows crystalline interplanar spacing of 0.185 nm that is

attributable to the (510) plane of $Ni_3(PO_4)_2$. Wide-angle XRD pattern of NiPPH shows a series of weak diffractions (Fig. S2, ESI†), which is resulted from very small size of nanoparticles with low crystallinity, assignable to nickel phosphate ($Ni_3(PO_4)_2$,
5 JCPDS No. 38-1473). A broad diffraction peak in the low-angle region indicates the presence of mesovoids with a poor periodicity.[8] The N_2 adsorption-desorption isotherms of NiPPH are of between type IV and type II (Fig. 2), with large hysteresis loops resembled H1-type, indicating the uniform mesoporosity.
10 The pore size distribution curve calculated by the NLDFT exhibits a narrow distribution with a maximum around 5.3 nm. The surface area and pore volume of NiPPH are 267 $m^2 g^{-1}$ and 0.191 $cm^3 g^{-1}$, respectively. Fractal analysis from the N_2 sorption isotherm was used to investigate the pore surface roughness of
15 the hybrid microspheres in terms of surface fractal dimension (D),[9] and D was calculated to be 2.866 (Fig. S3, ESI†). The high surface fractal dimension reveals that NiPPH possesses fine microstructure in the nanoscale through the hybrid microspheres, coinciding with the observations from SEM and TEM.
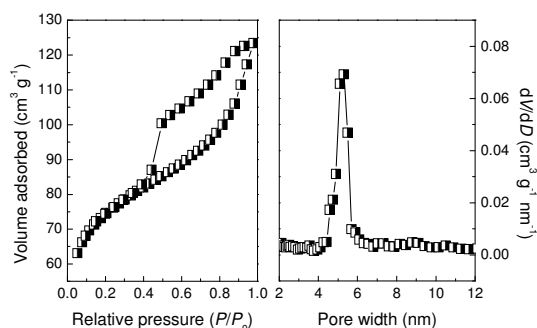

20

Fig. 2 N_2 adsorption-desorption isotherms of the NiPPH microspheres (*left*), and the corresponding NLDFT pore size distribution curve (*right*).

The typical bands of the NiPPH hybrid, such as P–O⋯Ni stretching vibrations (1053 cm^{-1}), C–N stretching (1312 cm^{-1}) and
25 asymmetric stretching vibration of O–P–O groups of phosphate (1276 cm^{-1}) can be observed in the FT-IR spectrum (Fig. S4, ESI†). Detailed characterizations of the hybrid network were further performed by TG-DSC, UV-vis. absorbance spectra and high-resolution XPS spectrum (ESI†). All the characterization
30 results reveal that the bridging ethylenephosphonic and phosphate moieties are present inside the NiPPH hybrid.

Fig. 3 Formation and preparation process of the NiPPH microspheres.

Thus, the hybrid microspheres are composed of not only
35 crystalline nickel phosphate but also amorphous nickel phosphonate, and the formation of crystalline $Ni_3(PO_4)_2$ nanoparticles played crucial roles in the formation of these microspheres. When phosphoric acid and nickel salts were mixed

under vigorous stirring, uncountable $Ni_3(PO_4)_2$ nanoparticles of a
40 few nanometers were emerged instantaneously. Nickel phosphonate clusters were formed after the addition of EDTMP to react with the rest of Ni^{2+}. These phosphonate clusters attached and wrapped the phosphate "nanoseeds" to generate core-shell-like secondary building blocks (SBB) under the driving of
45 intermolecular interaction, as depicted in Fig. 3. Thereafter, phosphate/phosphonate SBB would self-assembly to hierarchical hybrid microspheres to minimize the interfacial energy.[7] Distinct from the high solubility of nickel chloride, nitrate and sulfate in water, nickel phosphate is insoluble. If phosphoric acid was
50 substituted by hydrochloric, nitric, and sulphuric acids, the resultant products were amorphous nickel phosphonate nanoparticles (Fig. S8, ESI†). The hybrid microspheres could also be obtained when Na_2HPO_4, NaH_2PO_4, and Na_3PO_4 were employed as inorganic phosphors sources (Fig. S9, ESI†),
55 suggesting that $Ni_3(PO_4)_2$ involved in the self-assembly procedure. The selection of the right phosphonic precursors is considerably significant to determine the resultant micromorphology. In this study, the tetraphosphonic claw molecules containing pyridinic nitrogen could protonate in acid
60 environment and thus form zwitterions,[10] which could contribute for the hydrogen-bonding interactions between the phosphate nanoparticles and the slowly formed phosphonates. A kind of biphosphonic acid (HEDP, Fig. S1, ESI†) without pyridinic nitrogen component was tried to substitute EDTMP to prepare
65 hybrid microspheres, but failed, signifying the positive roles of proper weak interaction. Another N-containing phosphonic acid (BHMTPMP, Fig. S1, ESI†) with similar molecular structure to EDTMP but longer alkyl chains (-$[CH_2]_6$-) was used as well, and spherical nanoparticles were gained, which might be due to that
70 the strong hydrophobic interaction between the hexamethylenetriamine bridges could disturb the intermolecular interactions and the self-assembly process.[11]

CO_2 and heavy metal ions, mainly exhausted from industrial productions, have caused irreversible damages to the environment.
75 Adsorption by porous inorganic-organic hybrids has been proven to be an effective way to alleviate the damages, and it is reasonable to envision that the mesoporous NiPPH could perform as a host material for multiphase adsorption due to the low-cost, environmental friendly, hybrid network and well-defined
80 porosity. NiPPH shows the CO_2 uptake capacity of 1.86 mmol g^{-1} at 0 ℃ and 1 atm (Fig. S10, ESI†). This adsorption amount is much higher than microporous polymer ACMP-N (1.2 mmol g^{-1} at 0 ℃ and 1 atm).[12] The hybrid material can capture 1.45 mmol g^{-1} CO_2 under ambient conditions, which is much higher than
85 porous tin phosphonate (0.91 mmol g^{-1}, 25 ℃) with larger surface area of 723 $m^2 g^{-1}$.[13] The relatively high CO_2 adsorption capacity for NiPPH may be due to the well-defined mesoporosity and basic pyridine-type nitrogen in the organotetraphosphonic linkages.[1] Moreover, the adsorption capacity remains stable at
90 around 1.40 mmol g^{-1} even after multiple cycles, revealing the good recyclability of NiPPH for CO_2 capture. This is quite different from some lime-based CO_2 adsorbents,[14] the capacity of which decay continuously during multiple cycles due to an unavoidable carbonation conversion. The adsorption isotherms of
95 Pb^{2+}, Cu^{2+}, and Cd^{2+} ions by NiPPH are given in Fig. S11. The ions were almost quantitatively adsorbed until binding saturation

were reached, and the equilibrium adsorption capacity were determined to be 8.21, 7.35, and 7.18 mmol g^{-1} for Pb^{2+}, Cd^{2+}, and Cu^{2+} respectively. The Cu^{2+} uptake capacity is higher than previously reported Cu^{2+}-imprinted mesoporous silica with high surface area of 1203 m^2 g^{-1} (0.39 mmol g^{-1} for Cu^{2+}) and titanium phosphonate materials with surface area of 511 m^2 g^{-1} using hydroxyethylidene-bridged diphosphonate as linkage groups (2.21 mmol g^{-1} for Cu^{2+}).[15,16] The metal ion adsorption results indicate that not only the specific surface area but also the species of the phosphonic groups condensed in the hybrid framework are responsible for the improvement of ion binding capacities. The formation of chelating complexes due to the coordination of metal ions with defective P-OH and ethylene diamine bridging groups could be of great benefit to the high capacities of metal ion adsorption.
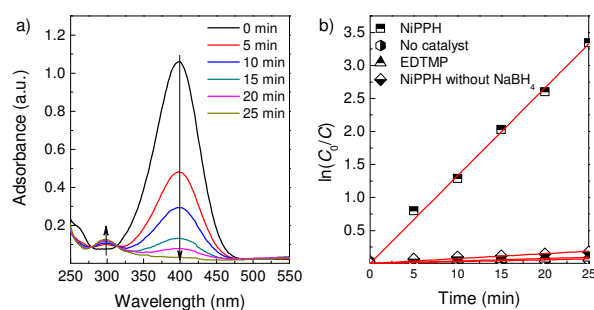

Fig. 4 (a) Time-dependent UV-vis. absorbance spectrum for the catalytic hydrogenation of 4-NP to 4-AP in the presence of NiPPH and NaBH$_4$. (b) Plot of ln(C_0/C) versus reaction time.

4-AP is a valuable industrial intermediate in manufacturing analgesic, antipyretic drugs, and anticorrosion lubricants, and noble metals are generally considered as efficient catalyst for the hydrogenation of 4-NP to 4-AP.[17] Recently, nickel nanosols synthesized by a microwave-assisted polyol method could be used to the catalytic hydrogenation of 4-NP to 4-AP, showing outstanding catalytic activity.[18] In this work, the NiPPH hybrid is the nanocomposite with organic and inorganic components connected on a molecular scale, possessing combined physicochemical characteristics of the two moieties. So it inspired us to apply the NiPPH hybrid to catalyze hydrogenation of 4-NP. As shown in Fig. 4, no reactions proceed in the absence of any catalysts or in the presence of only EDTMP even after 24 h. The concentration of 4-NP is hardly decreased in the presence of NiPPH but without NaBH$_4$, implying that the physical adsorption of 4-NP on NiPPH is negligible. However, the addition of NiPPH into the mixed solutions of 4-NP and NaBH$_4$ leads to gradual decoloration of the solution. According to the UV-vis. spectra (Fig. 4a), the adsorption of 4-NP at 400 nm decreases rapidly, accompanied with the increase of adsorption peak at 298 nm, which can be attributed to the generation of 4-AP. The presence of two isosbestic points situating at 277 and 315 nm signifies the successful transformation of 4-NP to 4-AP without producing byproducts.[17] This implies that the existence of Ni sites in the hybid can impel the occurrence of the reduction reaction. The reaction could be finished in 25 min, giving a rate constant k of 0.131 min^{-1}. Noticeably, the resultant catalytic activity of NiPPH is comparable with that of some noble metal catalysts (k = 0.148 min^{-1} under ambient conditions),[19] but the

relatively facile fabrication processes and low cost of the nickel phosphate/phosphonate hybrid make it promising in industrial production.

In summary, nickel phosphate/phosphonate hybrids were obtained by a simple phosphate-mediated strategy, which exhibited the first example of self-assembly synthesis of mesoporous non-siliceous organic-inorganic hybrid microspheres. The phosphonic groups were homogeneously incorporated into the organic-inorganic hybrid framework, exhibiting excellent capacities for capturing CO$_2$ and adsorbing heavy metal ions. The spherical hybrids showed outstanding catalytic activity for the reduction of 4-nitrophenol to 4-aminophenol with the assistance of NaBH$_4$ due to the presence of nickel active sites on the pore surface. This template-free method to prepare inorganic-organic hybrids provides a new route in nanomaterials synthesis science and presents potential in the environmental remediation and sustainable energy.

Notes and references

^{a} *Key Laboratory of Advanced Energy Materials Chemistry (Ministry of Education), Collaborative Innovation Center of Chemical Science and Engineering (Tianjin), College of Chemistry, Nankai University, Tianjin 300071, China. E-mail: zyyuan@nankai.edu.cn.*
^{b} *School of Chemical Engineering & Technology, Hebei University of Technology, Tianjin 300130, China.*
† Electronic supplementary information (ESI) available: Synthesis and detailed characterization. See DOI: 10.1039/x0xx00000x

1 T. Y. Ma and Z. Y. Yuan, *ChemSusChem*, 2011, **4**, 1407–1409.
2 J. E. Haskouri, C. Guillem, J. Latorre, A. Beltrán, D. Beltrán and P. Amorós, *Chem. Mater.*, 2004, **16**, 4359−4372.
3 M. Vallet-Regí, F. Balas and D. Arcos, *Angew. Chem. Int. Ed.*, 2007, **46**, 7548−7558.
4 T. Kimura and Y. Yamauchi, *Langmuir*, 2012, **28**, 12901−12908.
5 T. Kimura and Y. Yamauchi, *Chem. Asian J.*, 2013, **8**, 160−167.
6 T. Y. Ma and Z. Y. Yuan, *Dalton Trans.*, 2010, **39**, 9570−9578.
7 G. M. Whitesides and B. Grzybowski, *Science*, **2002**, 295, 2418−2421.
8 X. C. Wang, J. C. Yu, C. M. Ho, Y. D. Hou and X. Z. Fu, *Langmuir*, 2005, **21**, 2552−2559.
9 A. Du, B. Zhou, W. W. Xu, Q. J. Yu, Y. Shen, Z. H. Zhang, J. Shen and G. M. Wu, *Langmuir*, 2013, **29**, 11208−11216.
10 A. Cabeza, X. Ouyang, C. V. K. Sharma, M. A. G. Aranda, S. Bruque and A. Clearfield, *Inorg. Chem.*, 2002, **41**, 2325−2333.
11 X. B. Liu, Y. Yang and Q. H. Yang, *J. Mater. Chem. A*, 2013, **1**, 1525−1535.
12 H. Furukawa and O. M. Yaghi, *J. Am. Chem. Soc.*, 2009, **131**, 8875−8883.
13 A. Dutta, M. Pramanik, A. K. Patra, M. Nandi, H. Uyama and A. Bhaumik, *Chem. Commun.*, 2012, **48**, 6738–6740.
14 Y. Wang, Y. Q. Zhu and S. F. Wu, *Chem. Eng. J.*, 2013, **218**, 39−45.
15 C. C. Kang, W. M. Li, L. Tan, H. Li, C. H. Wei and Y. W. Tang, *J. Mater. Chem. A*, 2013, **1**, 7147−7153.
16 T. Y. Ma, X. Z. Lin, X. J. Zhang and Z. Y. Yuan, *New J. Chem.*, 2010, **34**, 1209–1216.
17 X. L. Fang, Z. H. Liu, M. F. Hsieh, M. Chen, P. X. Liu, C. Chen and N. F. Zheng, *ACS Nano*, 2012, **6**, 4434−4444.
18 M. Blosi, S. Albonetti, A. L. Costa, N. Sangiorgi and A. Sanson, *Chem. Eng. J.*, 2013, **215**, 616−625.
19 Y. Liu, Y. Fan, Y. Yuan, Y. Chen, F. Cheng and S. C. Jiang, *J. Mater. Chem.*, 2012, **22**, 21173–21182.

RSC Advances Accepted Manuscript